# Study on the Feasibility of Bacteriorhodopsin as Bio-Photosensitizer in Excitonic Solar Cell: A First Report

Velmurugan Thavasi[1], Tzvetana Lazarova[2], Slawomir Filipek[3], Michal Kolinski[3],
Enric Querol[4], Abhishek Kumar[5], Seeram Ramakrishna[1, 5, 6, *],
Esteve Padrós[2], and V. Renugopalakrishnan[7, *]

[1] *Nanoscience and Nanotechnology Initiative, National University of Singapore,
2, Engineering Drive 3, Singapore 117576, Singapore*
[2] *Unitat de Biofísica, Departament de Bioquímica i de Biologia Molecular, Facultat de Medicina,
and Centre d'Estudis en Biofísica, Universitat Autònoma de Barcelona, Barcelona, Spain*
[3] *International Institute of Molecular and Cell Biology, 4 Ks. Trojdena St, 02-109 Warsaw, Poland*
[4] *Institut de Biotecnologia i de Biomedicina, Universitat Autònoma de Barcelona, Barcelona, Spain*
[5] *Department of Mechanical Engineering, National University of Singapore, 9 Engineering Drive 1, Singapore 117576, Singapore*
[6] *Division of Bioengineering, National University of Singapore, 9 Engineering Drive 1, Singapore 117576, Singapore*
[7] *Children's Hospital, Harvard Medical School, 20 Shattuck Street, Boston, MA 02115, USA*

Bacteriorhodopsin (bR) is a membrane protein found in the archae *Halobacterium salinarum*. Here, we studied wild type bR and especially the triple mutant bR, 3Glu [E9Q/E194Q/E204Q], in combination with wide gap semiconductor $TiO_2$ for their suitability as efficient light harvester in solar cell. Our differential scanning calorimetry data show thermal robustness of bR wild type and 3Glu mutant, which make them good candidates as photosensitizer in solar cells. Molecular modeling indicates that binding of bR to the exposed oxygen atoms of anatase $TiO_2$ is favorable for electron transfer and directed by local, small distance interactions. A solar cell, based on bR wild type and bR triple mutant immobilized on nanocrystalline $TiO_2$ film was successfully constructed. The photocurrent density–photo voltage ($J$–$V$) characteristics of bio-sensitized solar cell (BSSC), based on the wild type bR and 3Glu mutant adsorbed on nanocrystalline $TiO_2$ film electrode were measured. The results show that the 3Glu mutant displays better photoelectric performance compared to the wild type bR, giving a short-circuit photocurrent density ($J_{SC}$) of 0.09 mA/cm$^2$ and the open-circuit photovoltage ($V_{OC}$) 0.35 V, under an illumination intensity of 40 mW/cm$^2$.

**Keywords:** Biosolar Cell, Photosynthesis, Energy Conversion, Metal Oxides, Dye Sensitized Solar Cells, Counter Electrode.

**RESEARCH ARTICLE**

## 1. INTRODUCTION

World energy needs are rapidly escalating and the major source of energy, the fossil fuels are declining at an astounding rate.[1] The cost of energy is on a rapid upward spiral. We have a deepening crisis on our threshold. Among the renewable sources of energy, sun's energy remains under utilized. Nature has crafted elaborate photosynthetic machinery for harnessing solar energy.[2] Photosynthetic machinery consists of a number of photoactive proteins, which harvest solar energy and synchronize their function to make photosynthesis very efficient. In the last few

decades, the solar cells, starting from silicon based materials have made slow, but gradual progress. An important milestone in the solar cells was the invention of excitonic solar cell called dye sensitized solar cells (DSSC).[3] In DSSC, light active synthetic dye (organic or organometallic) is usually bound to nanostructured wide gap metal oxide semiconductor and used as photo sensitizer to harvest the solar energy and generate excitons. Bio sensitized solar cell (BSSC) derives its inspiration from the relatively less understood and appreciated phenomenon of photon triggered electron ejection by a light activated proteins. DSSC and BSSC differ in the electron donor–synthetic (ruthenium II complex) dye in the former and

*Authors to whom correspondence should be addressed.

light-activated biomolecules in the later. Similar to DSSC, in BSSC the electron acceptor remains $TiO_2$ and ZnO in various morphologies. Investigations on the possibility of employing naturally occurring organic molecular materials in energy conversion devices for charge generation and separation had been on going for a long time, and especially focused on chlorophyll derivatives as the sensitizer in $TiO_2$ based solar cell.[4] Importantly the sensitizer for solar cell application should have thermal robustness and keep the functional activity for long—term while absorbing the solar radiation efficiently to produce photo-induced charge generation. Chlorophyll and its derivatives are considerably sensitive to extreme thermal conditions once extracted out of its source. Bacteriorhodopsin (bR), a natural light activated protein, which is found in *Halobacterium salinarum*, holds high promise for solar energy conversion.[5, 6] bR has remarkable functional stability against a high concentration of salt (up to 5 M NaCl) and thermal stability even up to ~140 °C, in dry state and with high quantum efficiency. In addition, bR functionally tolerates broad range of pH (5–11). It is easy and inexpensive to clone and express. Previously published reports on bR films, deposited on metals or metal oxides, were targeted for bio-optoelectronic applications.[7–9] Here, we report the construction of an excitonic solar cell based on bR triple mutant E9Q/E194Q/E204Q (3Glu) as photosensitizer. Furthermore, we studied the photoelectrical response of the constructed bio cell (bR/$TiO_2$ film) in response to light illumination. Molecular dynamic calculations were also carried out to describe the possible binding site of genetically engineered bR mutant onto the surface of $TiO_2$.

## 2. MATERIALS AND METHODS

### 2.1. The Design and Construction of Site Directed Mutant of bR

All single mutants were obtained by PCR site-directed mutagenesis and amplified in the *E. coli* TG1 strain as described previously.[10] The gene coding for bacteriorhodopsin, bop gene, subcloned in pUC119 as a 1.2 Kb BamHI/HindIII fragment and was used as a template for the mutagenesis. After screening the mutants by DNA sequencing, they were transformed and expressed in *H. salinarum* L33 strain using shuttle plasmid pXLNovR.[a] The multiple mutants were constructed by cloning the single mutants together, taking advantage of unique restriction sites. Purple membranes (PM) were grown and purified by standard methods.[10] The mutations were confirmed from *H. salinarum* transformants by sequencing the bop gene from isolated DNA. UV-Vis absorption of bR in Tris buffer at pH 8.8 of concentration 30 $\mu$M was recorded using Thermo Spectronic Unicam UV 300 spectrophotometer.

---

[a]Kindly provided by Dr. R. Needleman (Wayne State University, Detroit, MI USA).

### 2.2. Hydroxylamine Reaction

The hydroxylamine bleaching of bR was performed as described previously[11] to measure the chemical stability. Briefly, membrane suspensions (at about $1.5 \times 10^{-5}$ M bR) were reacted with 1 M hydroxylamine in 150 mM sodium phosphate at pH 7.0. The illumination of the samples was done by using white light of 300 lux, equipped with the heat filter.

### 2.3. Differential Scanning Calorimetry (DSC)

DSC measurements were carried out on a MicroCal MC2+ instrument (MicroCal, Northhampton, MA) to measure the temperature stability of bR. The purple membrane samples were first dialyzed overnight against water and subsequently were introduced into the cell holder with a final concentration at about 2 mg/ml of bR. The reference cell was loaded with the aqueous medium obtained from the dialysis of the purple membrane suspension. The data were collected in the temperature range from 25 °C to 110 °C and at heating rate of 90 °C/h. A pressure of 1.7 atm of $N_2$ was applied to the cells in order to avoid an ebullition of the samples at higher temperatures. After the first scan was completed, each sample was cooled to 25 °C and reheated again to check reversibility. The chemical baselines were constructed and subtracted as described by Takahashi and Sturtevant.[12]

### 2.4. Theoretical Study

Computational studies were carried out to model the binding process of individual amino acids to the crystal 1 0 0 and 1 0 1 facets of $TiO_2$ using DFT with B3LYP functional employing 6-31G* basis set (Gaussian program, v.03 rev. C.02 Gaussian Inc., Pittsburgh, PA, USA). Crystal structures of anatase $TiO_2$ (Ref. [13]) were used for the calculations. Initial structural coordinates of bR were taken from the Protein Data Bank code id = 1C3W,[14] corresponding to the X-ray crystal structure, at 1.55 Å resolution, of the wild-type bR (wt) in the ground state. Missing residues were modeled according to another crystal structure of bR (code id = 1BRR),[15] determined at a lower resolution 2.9 Å but contains more residues 3–232. This is especially important for the electrostatic potential since C-terminus of bR contains charged residues. The whole structure of bR and its mutants were modeled in Yasara v. 7.9 (YASARA Biosciences) using Yamber2 forcefield (modification of Amber 99 forcefield). Visualization of electrostatic potential on molecular surfaces of bR was also done in Yasara.

### 2.5. Preparation of NanoTiO$_2$ Film

Nanoparticles of $TiO_2$ (P-25, 30 nm, Degussa, Essen, Germany) were used as the electron acceptor (anode). 0.5 g of $TiO_2$ nanoparticles (NPs) were dispersed in 20 ml

of equal volume of ethanol and methanol and obtained as colloidal solution after stirring for 15 min. The nanocrystalline TiO$_2$ film was prepared by a similar procedure as described in our previous work.[16] The TiO$_2$ nanoparticles dispersion was sprayed using an air-brush on top of the fluorine-doped tin oxide (FTO) conducting glass at room temperature and the film was then allowed to dry in air for 30 min. The active area of the electrode was typically 0.5 cm$^2$. The TiO$_2$ nanoparticulate film was then heated at a rate of 5 °C min$^{-1}$ up to 450 °C and sintered at 450 °C for 1 h. The thickness of the TiO$_2$ nanoparticulate ceramic film on FTO was determined as about 15 $\mu$m.

### 2.6. Immobilization of bR onto NanoTiO$_2$ Film

Immobilization of bR onto TiO$_2$ was tested in two steps. Step one was aimed towards investigating the effect of mutant on the photoelectric performance. In the first step, a sintered TiO$_2$ nanocrystalline ceramic film was immersed in 1.5 ml of 4 mg/ml wt bR solution. Similarly, another ceramic TiO$_2$ film was immersed in 1.5 ml of 4 mg/ml triple mutant (3Glu) bR at pH 7 for 12 h at 22 °C.

The second step (step 2) was aimed towards determining the effective binding of the 3Glu bR onto the surface of TiO$_2$ nanofilm in order to improve the photoelectric performance of 3Glu bR, which involved several stages of surface treatment. The sintered TiO$_2$ nanocrystalline ceramic films were first introduced into a smaller petri dish containing a solution of 0.1 M of 1-ethyl-3(3-dimethylaminopropyl)carbodiimide (EDC) and 0.08 M of N-hydroxy succinimide (NHS) prepared in MES buffer at 5 °C and soaked for 1 h. Then the FTO/TiO$_2$ ceramic film was then transferred into the 1.2 ml of PBS buffer solution (pH 8.8), then 500 $\mu$l of 4 mg/ml concentration of triple mutant bR was added and kept under mild stirring for 12 h at 22 °C. The best binding of bR onto the surface of nanoTiO$_2$ film (pink color appearance of film) was achieved after 12 h of treatment.

In both the steps one and two, the nanoparticulate films after the surface treatment with wt bR and 3Glu bR were taken out and washed off gently with deionized water to ensure that there is no unbound or loosely bound bR on the surface of TiO$_2$ film and then dried overnight under vacuum. The resultant setup was denoted as FTO/TiO$_2$/bR and acted as working electrode. The counter electrode was prepared by depositing a transparent thin film of aluminum onto FTO conductive surface by sputtering and to an area of 0.5 cm$^2$. The corrosion stability of the Al/FTO in the electrolyte solution was examined in our study. No color change of electrolyte, or no cracking and deformation of the Al film on FTO were noticed even after 1 week. These results indicated that Al coating was stable in the electrolyte.

### 2.7. Photovoltaic Cell Assembly and Measurements

The working electrode (FTO/TiO$_2$/bR) and the counter electrode (FTO/Al) were sandwiched together to make cell. Another cell was constructed in a similar fashion except that bR was excluded i.e., working electrode has only FTO/TiO$_2$ and used as control. A solution containing 0.1 M lithium iodide, 0.03 M I$_2$, and 0.5 M KCl was prepared in Tris buffer with pH 8 and used as a redox electrolyte. 200 $\mu$l of the electrolyte was injected slowly into the cell. Photocurrent measurements of the assembled cell were conducted under irradiation of 40 mW/cm$^2$ using xenon lamp (Thermo Oriel Xenon Lamp 150 W: Model 66902). Current density–voltage curves of assembled biosensitized solar cell were obtained by using a potentiostat (PGSTAT30, Autolab PGSTAT30, Eco Chemie B.V., and The Netherlands).

## 3. RESULTS AND DISCUSSION

### 3.1. Structural Arrangement of 3Glu Mutant bR

The structure of the triple mutant of bR is shown in Figure 1. Four Glu side chains (Glu9, Glu74, Glu194 and Glu204) are located in the extracellular region of the protein. Two of these residues Glu194 and Glu204 together with water cluster were identified as major players in the proton release mechanism.[17] Moreover, it has been shown previously that the mutation of either of these Glu to Gln strongly impairs not only their function, but also the structure of the protein.[18] The mutation of the two other Glu residues, Glu9 and Glu74, located in the extracellular region does not impair proton release kinetics and photocycle kinetics, suggesting that they are not implicated in the functioning of bR.[19] The mutation of three of EC Glu residues (Glu9, Glu194 and Glu204) for Gln (E9Q/E194Q/E204Q) results in 3Glu protein with less negative charge density at the extracellular surface, which
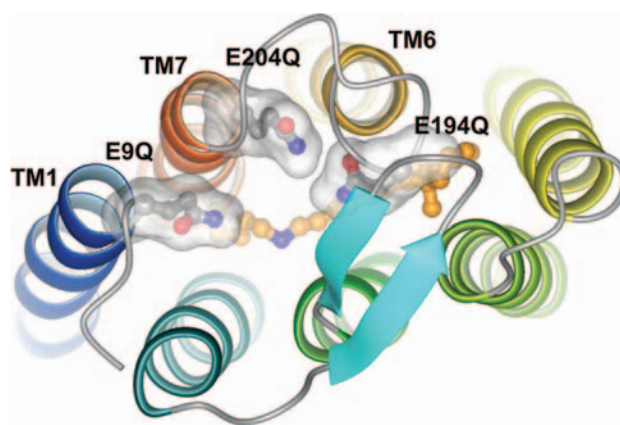


**Fig. 1.** Extracellular region of 3Glu mutant of bR. The three Glu residues mutated to Gln are shown in separated transparent surfaces. Retinal and Lys216 carbon atoms are colored in orange. Two pdb structures were combined as stated in the methods section.

could facilitate more favorable binding of bR to the TiO$_2$ surface via electrostatic interactions.

## 3.2. Thermal Denaturation Experiments

Thermal robustness of the biomaterial is a pre-requisite for it photovoltaic application. Therefore, the thermal stability of the single EC (extracellular) Glu mutants, composing 3Glu mutant was studied by performing DSC experiments. It is well known that the thermogram of native purple membrane (PM) consists of a two main transitions. The irreversible transition at ~98 °C, is accounted for the destruction of the helical interactions within the protein and retinal release, while a smaller reversible pretransition, presumably arising from the re-organization of the hexagonal paracrystalline arrangement.[20] Figure 2 compares the thermal transitions temperatures (Tm), obtained by DSC measurements of wild type (wt) bR and the mutants. The comparison of the thermal transitions gives the following order: E194Q > E9Q > E204Q > 3Glu, with the single E194Q mutant displaying a similar thermal stability as wild type bR. Though the rest of Glu bR mutants display somehow lower Tm, compared to wt bR, these changes are not dramatic, because the Tm does not go beyond 94 °C. The lack of the pre transition in the 3Glu mutant could be accounted for the lower pre-transition temperatures, recorded for the single E9Q, E194Q and E204Q mutants, composing the triple mutant.

## 3.3. Hydroxylamine Reaction

The bR mutants were examined by the hydroxylamine reaction to test their stability to the chemical reagents. For wt bR, it is well established that the hydroxylamine ruptures the Schiff base linkage between the retinal and Lys216 resulting in a decreases of the absorption maximum at 568 nm and appearance of a band at about 330 nm due to retinaloxime.[10] The change in the intensity of the
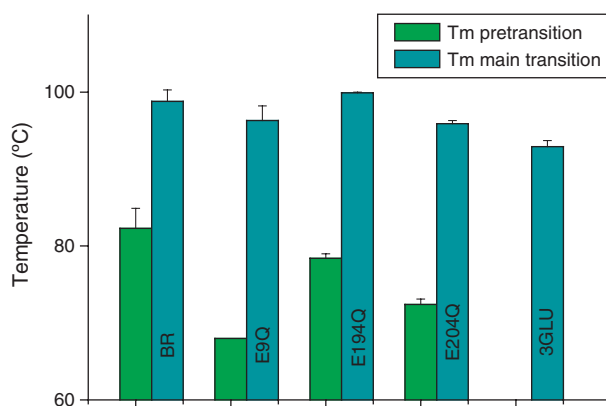
absorption maximum at 570 nm, as a function of the time is used to measure the loss of the native structure of bR. Figure 3(a) shows the kinetics of the bleaching of wt bR and the single Glu mutants, and 3Glu mutants. Figure 4 compares the half time for the bleaching of the Glu bR mutants and wt, in the presence of hydroxylamine and light. The presented data demonstrate that the Schiff base of all mutants is more accessible to hydroxylamine than wt bR, implying that these residues are important in the helical displacement and compactness of protein structure during the photocycle. Moreover, these finding imply that care should be taken to avoid the presence of any compound with similar reactivity as hydroxylamine in the medium, constituting the solar cell.

## 3.4. Theoretical Studies of the Interaction of bR Mutant with TiO$_2$ Surface

Molecular modeling of the structure of bacteriorhodopsin (bR) and its mutants including interactions with inorganic surfaces can provide energetically favorable orientations of bR mutants on the surface of TiO$_2$. Computational studies were carried out for modeling the binding process of bR to crystal surfaces of TiO$_2$. Our computational study showed that there is a possibility of preferential binding of bR to the TiO$_2$ anatase surface 1 0 0 (or identical by symmetry the 0 1 0 surface) via positively charged arginine and lysine amino acid residues located at cytoplasmic surface of protein. The TiO$_2$ surfaces exhibit small grooves formed by oxygen atoms on both sides. Such exposed oxygen atoms are located in an alternating pattern and form triangles well suited for binding of positively charged residues of bR. A similar pattern was observed for the more thermodynamically stable 101 facet of TiO$_2$. Both the extracellular and cytoplasmic sides of bR contain exposed charged residues. However, there are only few such residues on the extracellular side (N-terminus)
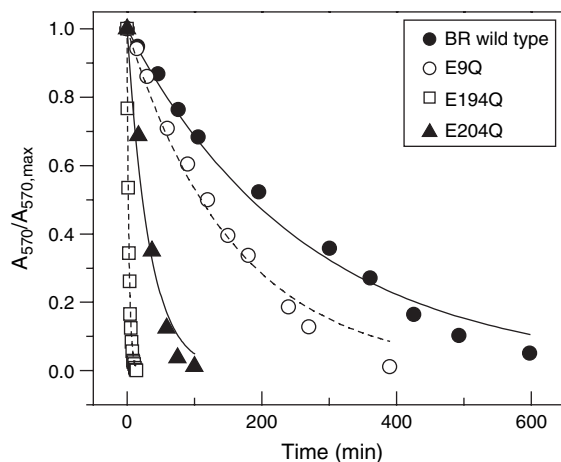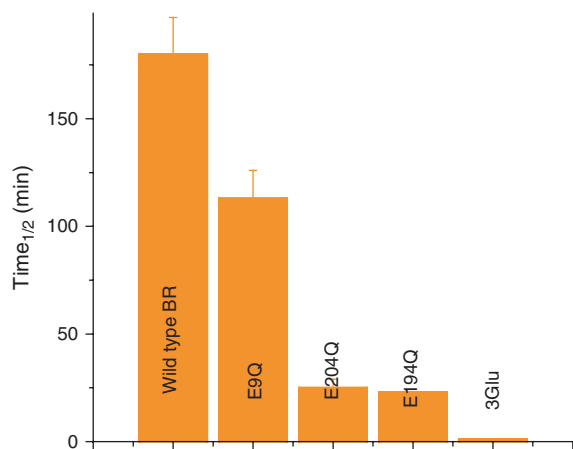
**Fig. 2.** The thermal transitions temperatures (Tm) of wild type bR and bR mutants, obtained by DSC measurements, as described in materials and methods.

**Fig. 3.** The rate of hydroxylamine reaction with wild type bR and single Glu mutants of bR, as measured by the absorbance changes at 570 nm. The reaction was carried out in presence of light.

**Fig. 4.** Comparison of the half-time of the bleaching for bR and bR mutants in the presence of 1 M hydroxylamine in 150 mM sodium phosphate at pH 7.0 and light intensity of 300 lux.

and 14 (seven positively charged: K30, K40, K41, K159, R164, R225, R227; and seven negatively charged: D36, D38, D102, D104, E161, E166, E232) on the cytoplasmic side (C-terminus).[15] Positively charged residues can bind to exposed oxygen atoms of anatase surface directly in neutral or basic environments when this surface is covered by negatively charged hydroxyl groups from solution. The exposed oxygen atoms at groove edges can electrostatically interact with positively charged bR residues. At the acidic pH, when the oxygen atoms on the crystal surface are saturated by protons from solution, the positively charged residues from cytoplasmic side of bR are able to bind to anatase surface. The isoelectric point of $TiO_2$ is 6.0 and its surface is therefore nearly neutral, or covered with a small amount of –OH groups bound to Ti, at neutral pH. The electrostatic potential map of bR (Fig. 5(b)) is different from the image based on surface charged amino acids only (Fig. 5(a)) because the internal charged residues also contribute to electrostatic potential. It can be observed that a negatively charged spot is located close to the entrance to bR just below a beta-sheet (Fig. 5(b)). In case of 3Glu mutant (Fig. 5(c)) extracellular part of bR is widely altered whereas cytoplasmic part is nearly the same. Electrostatic potential of cytoplasmic surface of bR is mostly negatively charged and mutations of residues located at extracellular side have no effect on it although the overall charge of bR has increased by three. Negatively charged surface would suggest precluded binding of bR to anatase crystal with exposed and also negatively charged oxygen atoms, however, such binding is directed by local, small range interactions so positively charged residues (seen as blue spots at Fig. 5(a)) are able to bind to oxygen atoms on the crystal surface. Depending on electrostatic potential of the crystal surface (changing with pH) the negatively or positively charged residues on the surfaces of bR would be able to bind to anatase.
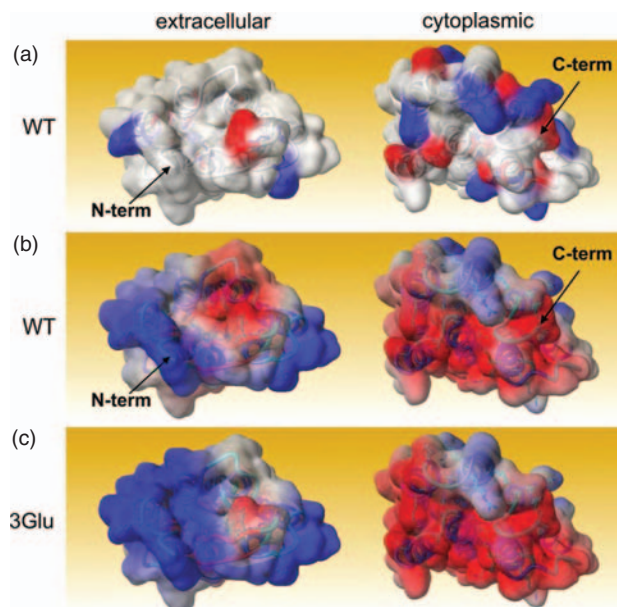


**Fig. 5.** Extracellular and cytoplasmic surfaces of bR. (a) The molecular surface of wt bR is colored by charged amino acids—positively charged in blue and negatively charged in red. (b) The electrostatic potential map of wt bR. (c) The electrostatic potential map of 3Glu mutant of bR. Positive potential shown in blue color and negative potential in red.

### 3.5. Photoelectric Performance of bR in Solar Cell

Figure 6 compares the absorption spectra of the bR and the N3, a successfully and widely used synthetic dye sensitizer[21] used in DSSC, measured in Tris buffer and ethanol solution respectively. N3 dye shows two absorption bands at 396 nm and 538 nm, respectively. However, for the same concentration of 30 $\mu$M, the absorption intensity of the bR is about two times stronger than the value of N3 dye. The lowest unoccupied molecular orbital (LUMO) and highest occupied molecular orbital (HOMO) of bR were determined in the literature to be $-3.8$ eV
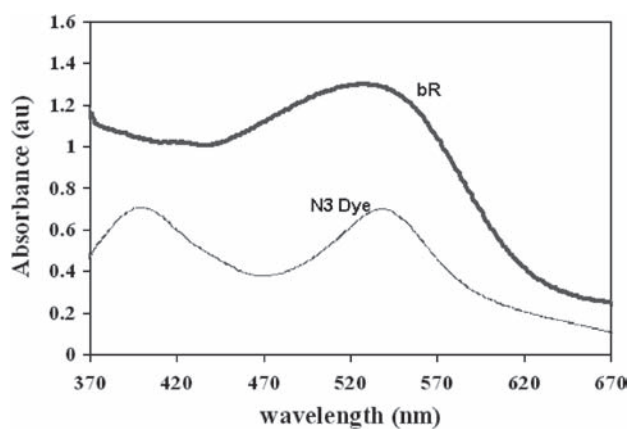


**Fig. 6.** UV-Vis absorption spectra of 30 $\mu$M of 3Glu (triple mutant) bacteriorhodopsin (bold line) in Tris buffer, pH 8.8 and N3 dye in ethanol (thin line) were recorded at room temperature using Thermo Spectronic Unicam UV 300 spectrophotometer.

RESEARCH ARTICLE

and $-5.2$ eV, respectively using surface photovoltage spectroscopy (SPS).[22] The conduction band ($E_C$) energy of TiO$_2$ is $-4.2$ eV. The TiO$_2$/bR system therefore, is energetically favorable for electron injection and transport. It is also well known that protonation of surface oxohydroxyl groups present on the surface of nanosized TiO$_2$ alters significantly the flat band potential of the oxide itself.[23] Schematic of the energy diagram for TiO$_2$/bR is given in Figure 7. To investigate the effect of the mutation with wild type, the bio-sensitized solar cells were assembled using wild type bR and triple mutant type bR bound TiO$_2$ films prepared as mentioned in the step one of method Section 2.6. The schematic diagram of the assembled BSSC is shown in Figure 8. The photocurrent measurements of the assembled cells were carried out. The $J$–$V$ characteristic curves are shown in the Figure 9. The triple mutant bR (3Glu) adsorbed nanocrystalline TiO$_2$ film electrode solar cell produced a short-circuit photocurrent density ($J_{SC}$) of 0.038 mA/cm$^2$ whereas wild type bR adsorbed TiO$_2$ cell showed only 0.0269 mA/cm$^2$ as $J_{SC}$. However, for both the type of bR, the open-circuit photovoltage ($V_{OC}$) was about 0.39 V. The experiment was carried out using FTO/bR alone as blank cell to ensure that there was no artifact and confirmed that no photoelectric effect was observed from FTO/bR. It indicates that TiO$_2$/bR is clearly responsible for photoelectric effect and was due to the photoactive layer of nanoparticulate TiO$_2$ and mainly their higher surface area. The photoelectric performance of TiO$_2$/bR was also confirmed by testing at the dark current condition and on–off condition. The tested performance of 3Glu bR is shown in Figure 10. The experimental results confirmed that both wt bR and 3Glu bR respond to the light illumination, however, the triple mutant (3Glu) showed up better photoelectric performance ($J_{SC}$ of 0.038 mA/cm$^2$) compared to wild type bR (0.0269 mA/cm$^2$), which is likely due to more efficiently assembling and binding nature of the mutated protein (3Glu) to the TiO$_2$. Indeed, the elimination of three negative charged Glu residues (E9, E194 and E204) from
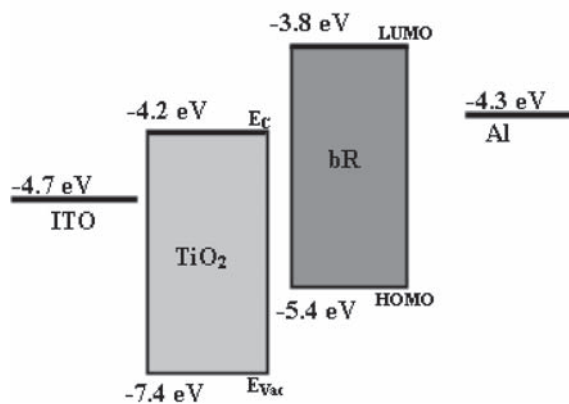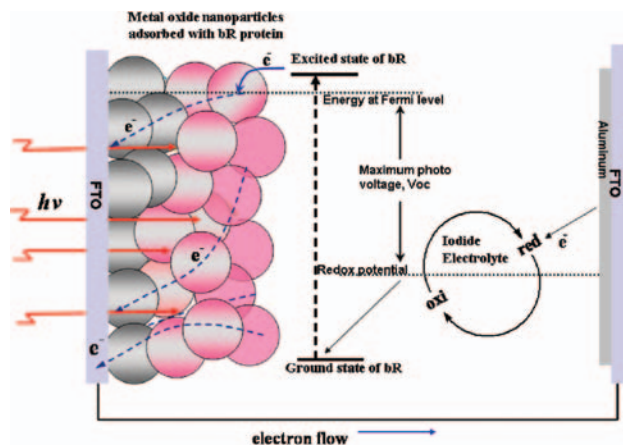


**Fig. 8.** Schematic of Bio-Sensitized Solar Cell (BSSC). Spherical TiO$_2$ nanoparticles are immobilized with bR act as working electrode i.e., FTO/TiO$_2$/bR and the counter electrode is made with FTO/Al. The working electrode is percolated with an electrolyte (0.1 M LiI, 0.03 M I$_2$, and 0.5 M KCl in Tris buffer of pH 8). Photocurrent generates upon illumination of bR bound TiO$_2$ and transported into the TiO$_2$ nanoparticulate matrix for the collection.

EC site of BR strongly changes the surface potential map of the protein (Fig. 5), which most likely facilitates the binding of 3Glu to TiO$_2$. Nevertheless, we noticed that the current density was poor for 3Glu bound TiO$_2$ prepared under step one of immobilization method.

To analyze if the process conditions such as pH and the nature of medium such as buffer surface could play any role in binding of protein molecules onto the surface of TiO$_2$, in the following experiments 3Glu bR bound TiO$_2$ film that was prepared under new optimized condition (as described in step two of method Section 2.6) to assemble the solar cell. Photocurrent measurements of the assembled bio-sensitized solar cell using 3Glu bR/TiO$_2$ and the control cell were conducted and the characteristic curves



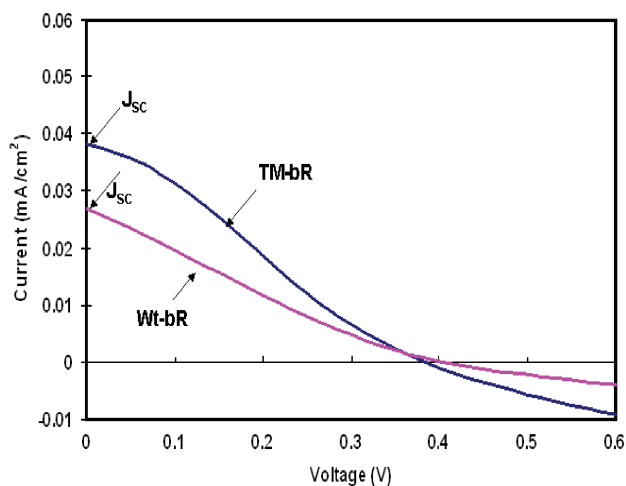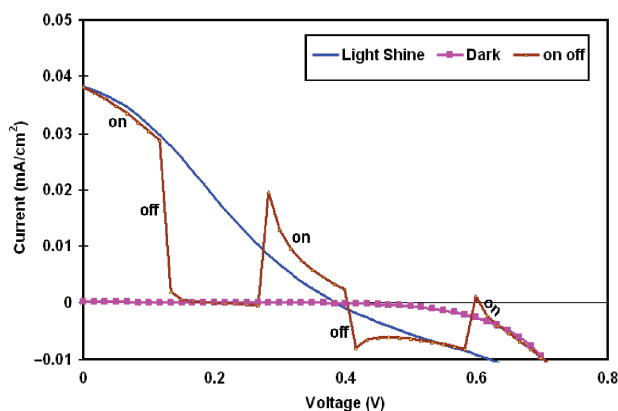**Fig. 7.** Schematic of energy diagram of bR/TiO$_2$ based bio-sensitized solar cell.



**Fig. 9.** Photocurrent–photovoltage ($J$–$V$) characteristics of BSSC based on the wild type bR (pink color) and 3Glu bR (blue color) adsorbed on nanocrystalline TiO$_2$ film electrode. The light intensity was 40 mW/cm$^2$.

**Fig. 10.** Photocurrent–photovoltage ($J$–$V$) characteristics of 3Glu mutant/nanocrystalline TiO$_2$ based BSSC tested under dark condition (pink line), on and off condition (brown line) of the illumination of 40 mW/cm$^2$.

are shown in the Figure 11. The photoelectric response of 3Glu mutant immobilized on TiO$_2$ nanoparticulate film based cell in response to light (Fig. 11(A)) is compared to the control cell which does not have bR for sensitization (Fig. 11(B)).

Upon surface treatment and assembly in such way, the bR immobilized nanocrystalline TiO$_2$ film electrode solar cell produced a short-circuit photocurrent density ($J_{SC}$) of 0.089 mA/cm$^2$ and the open-circuit photovoltage ($V_{OC}$) of 0.35 V under an excitation intensity of 40 mW/cm$^2$. These data imply that the pH and buffer composition play an important role in mediating the bR for effective surface binding onto TiO$_2$. As known, upon illumination bR undergoes photocycle, during which bR pumps a proton from the intracellular to the extracellular side (EC) of the membrane. Therefore the photocurrent generation in solar cell could be, as indicated by Terasaki et al.,[24] due to the
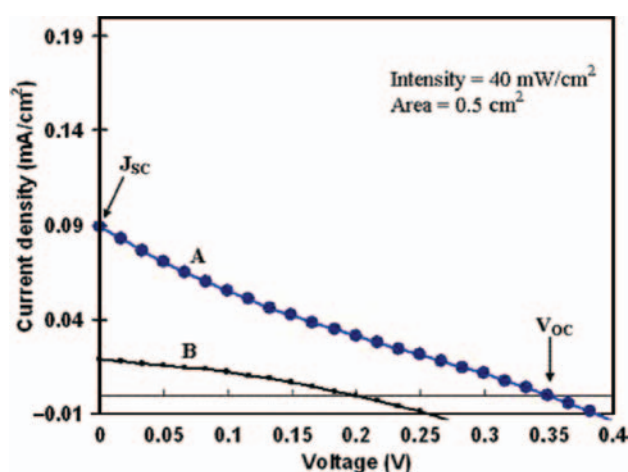


**Fig. 11.** Photocurrent–photovoltage ($J$–$V$) characteristics of BSSC based on the 3Glu mutant immobilized under optimized binding condition on nanocrystalline TiO$_2$ film electrode. (A) OTE/ TiO$_2$/bR/I$_2$/Al and (B) OTE/TiO$_2$/electrolyte/Al as control. The light intensity was 40 mW/cm$^2$.

formation of transmembrane electrochemical gradient that leads to charge separation during the photocycle of bR.

Platinum (Pt) has been used widely as counter electrode for iodide regeneration due to its potential and greater catalytic activity, which lead to higher energy conversion efficiency.[25, 26] Miyasaka et al.[27] have used Pt for deposition of bR. One of the objectives of bio-sensitized solar cell (BSSC) is to make it cost effective and hence the substitution of Pt by Al was attempted in the studies reported here. It is worthwhile to mention that the cost of aluminum (Al) is about 75% cheaper than platinum. The thermal conductivity of Al is 237 W/m-K whereas for Pt, it is 71.6 W/m-K. As the thermal conductivity of Al is higher, the bio-solar cell should be able to reach thermal equilibrium at a much faster rate with the surroundings than Pt when exposed to sun light for longer period of time and hence, considering the durability and stability of the BSSC, using Al as counter electrode is expected to reduce the possibility of severe impairment of the light harvesting proteins as well as liquid iodide electrolyte. Moreover, it was found in the literatures that platinum-containing compounds could denature DNA,[28] hemoglobin[29] and platinum electrode induce proteins for agglomeration or adsorption onto Pt electrode when pH or temperature was varied.[30, 31] bR being a protein, a similar effect could be occurred. Al, being an excellent corrosion resistance metal, has also been successfully used as counter electrode in organic solar cells to prevent from oxidation.[32] Therefore, this study was designed with safer, but quite effective and cheaper Al metal as an alternate counter electrode.

To our knowledge, this is the first report demonstrating the fabrication of protein sensitized solar cell as BSSC and establishing that bR is involved in photo induced charge transfer into the ceramic metal oxide semiconductor upon effective immobilization on the TiO$_2$ surface.

Kay et al.[33] demonstrated an open circuit photovoltage ($V_{OC}$) of 0.52 V and a short circuit current density ($J_{SC}$) of 9.4 mA/cm$^2$ for 1 cm$^2$ area of chlorophyll sensitized TiO$_2$ based BSSC under 100 mW/cm$^2$. Similarly, Amao et al.[34] obtained 0.305 mA/cm$^2$ as $J_{SC}$ and 0.426 V as $V_{OC}$ for 4 cm$^2$ area of chlorophyll sensitized TiO$_2$ based BSSC for the irradiation of 80 mW/cm$^2$. The TiO$_2$ based BSSC, using chlorophyll as the bio-sensitizer, showed better performance compared to the value ($J_{SC}$ as 0.089 mA/cm$^2$ for 0.5 cm$^2$ at 40 mW/cm$^2$) that we obtained for bR sensitized BSSC. However, it should be noted that this study did not really attempt on the site-specific bR binding onto the TiO$_2$, which could be one possible reason for the lower performance of bR based BSSC. It is also important to mention that literatures implemented with selective-site binding of bR onto materials for bio-optoelectronic applications reported better photoelectric generation. For example, the selective-site electrodeposition of bR onto the surface of gallium arsenide (GaAs) produced photo induced current of about 1.7 mA in field effect transistor (FET) device under the irradiation of 40 mW/cm$^2$

**RESEARCH ARTICLE**

light intensity.[35] Likewise, bacteriorhodopsin oriented by an electric field of 20–40 V/cm onto the -silicon *n*-channel metal-oxide based FET device delivered a response of 4.7 mA/W.[35] Similarly, Nicolini et al.[36] demonstrated a photoresponse of 5 mA for oriented bR/ITO based device. All these studies suggest that the preferential molecular orientation of bR towards $TiO_2$ film could be an important factor in obtaining larger photo current out of bR in solar cells and most likely could surpass the performance of other bio-sensitizer such as cholorophyll, if highly oriented bR is achieved. Thus, our ongoing research is focused on studies of preferential orientation bR to $TiO_2$. It is also realized that Al electrode has higher potential for the iodide/triiodide redox couple. In our ongoing study, we are investigating carbon/graphite as counter electrode that may result in substantial improvement in the overall performance of BSSC. Furthermore, we are trying to get insight of physical mechanism of charge generation in bR and electron injection into $TiO_2$.

## 4. CONCLUSION

In conclusion, our results show that the designed 3Glu mutant (triple mutant) display good stability against high temperature. However, the elevated sensitivity of 3Glu mutant to the hydroxylamine under illumination, make obvious that similar reagents should be avoided while designing the bio-solar cell. Importantly, as we have reported previously, the 3Glu mutant has preserved proton pumping activity and photocycle and enhanced thermal and chemical stability in the presence of ions.[37] The elimination of the three negative charges from EC site of bR strongly changes the surface potential map of the protein. The extracellular surface of 3Glu mutant is exposed only by E74 residue, which might facilitate favorable binding to $TiO_2$. Indeed, the computational study indicates that the electrostatic potential map of 3Glu shows better likelihood to bind efficiently to $TiO_2$. These finding are in correlation with higher photoelectric response of the solar cell composed by the triple mutant (3Glu) bR than that composed by the wild type bR. To our knowledge, this is the first demonstration by fabricating a typical solar cell that the bR is involved in photo induced charge transfer onto the ceramic metal oxide semiconductor upon immobilization. We believe that bR can be a better current-generating component in solar devices, upon further improving its structural property through rational protein engineering, as well as it binding property by implementing orientation or electro-active linker molecules. Both lines of the studies are already underway in our laboratories. By the aid of such investigation and design, bR can be fully realized as an efficient bio-photosensitizer to obtain the maximum solar energy-electrical energy conversion efficiency and provide an environmentally benignant "green" alternate to Ru dyes.

## ABBREVIATIONS

DSSC    Dye sensitized solar cell,
BSSC    Bio sensitized solar cell,
DSC     Differential scanning calorimetry,
bR      Bacteriorhodopsin,
Wt      Wild type,
3Glu    [E9QE194Q/E204Q],
N3      *cis*-bis isothiocyanato bis 2,2-bipyridyl-4,4-dicarboxylato-ruthenium II dye.

## References and Notes

1. http://www.worldenergyoutlook.org/.
2. (a) R. van Grondelle and I. N. Vladimir, *Phys. Chem. Chem. Phys.* 8, 793 (**2006**); H. Lee, Y.-C. Cheng, and G. R. Fleming, *Science* 316, 1462 (**2007**); (b) M. Yang and G. R. Fleming, *Chem. Phys.* 282, 161 (**2002**); (c) G. S. Engel, T. R. Calhoun, E. L. Read, T.-K. Ahn, T. Mancal, Y.-C. Cheng, R. E. Blankenship, and G. R. Fleming, *Nature (London)* 446, 782 (**2007**).
3. B. O'Regan and M. Graetzel, *Nature (London)* 353, 737 (**1991**).
4. (a) H. Tributsch and M. Calvin, *Photochem. Photobio.* 14, 95 (**1971**); (b) H. Tributsch, *J. Theor. Biol.* 52, 17 (**1975**).
5. A. LaVan David and N. Cha Jennifer, *Proc. Natl. Acad. Sci. USA* 103, 5251 (**2006**).
6. P. Bertoncello, D. Nicolini, C. Paternolli, V. Bavastrello, and C. Nicolini, *IEEE Trans. Nanobiosci.* 2, 124 (**2003**).
7. K. Clays, S. Van Elshocht, and A. Persoons, *Opt. Lett.* 25, 1391 (**2000**).
8. Y. Saga, T. Watanabe, K. Koyama, and T. Miyasaka, *J. Phys. Chem. B* 103, 234 (**1999**).
9. K. Koyama, N. Yamaguchi, and T. Miyasaka, *Adv. Mater* 7, 590 (**1995**).
10. C. Sanz, T. Lazarova, F. Sepulcre, R. Gonzalez-Moreno, J.-L. Bourdelande, E. Querol, and E. Padros, *FEBS Lett.* 456, 191 (**1999**).
11. D. Oesterhelt, L. Schuhmann, and H. Gruber, *FEBS Lett.* 44, 257 (**1974**).
12. C. G. Brouillette, D. D. Muccio, and T. K. Finney, *Biochemistry* 26, 7431 (**1987**).
13. M. Wagemaker, J. K. Gordon, A. Van Well Ad, H. Mutka, and M. M. Fokko, *J. Am. Chem. Soc.* 125, 840 (**2003**).
14. H. Luecke, B. Schobert, H. T. Richter, J. P. Cartailler, and J. K. Lanyi, *J. Mol. Biol.* 291, 899 (**1999**).
15. L. Essen, R. Siegert, W. D. Lehmann, and D. Oesterhelt, *Proc. Natl. Acad. Sci. USA* 95, 11673 (**1998**).
16. K. Fujihara, A. Kumar, R. Jose, S. Ramakrishna, and S. Uchida, *Nanotech.* 18, 365709/1 (**2007**).
17. F. Garczarek, S. B. Leonid, K. L. Janos, and K. Gerwert, *Proc. Natl. Acad. Sci. USA* 102, 3633 (**2005**).

**18.** T. Lazarova, C. Sanz, E. Querol, and E. Padros, *Biophys. J.* 78, 2022 **(2000)**.

**19.** E. Padrós, C. Sanz, T. Lazarova, M. Márquez, F. Sepulcre, X. Trapote, F. J. Muñoz, L. Bourdelande, E. Querol, *NATO Science Series I: Life and Behavioral Sciences* 335, 350 **(2001)**.

**20.** C. Sanz, M. Marquez, A. Peralvarez, S. Elouatik, F. Sepulcre, E. Querol, T. Lazarova, and E. Padros, *J. Biol. Chem.* 276, 40788 **(2001)**.

**21.** K.-J. Jiang, J.-b. Xia, N. Masaki, S. Noda, and S. Yanagida, *Inorg. Chimi. Acta.* 361, 783 **(2008)**.

**22.** L. S. Li, T. Xu, Y. J. Zhang, J. Jin, T. J. Li, B. Zou, and J.-P. Wang, *J. Vacuum Sci. Technol. A* 19, 1037 **(2001)**.

**23.** (a) K. Kalyanasundaram and M. K. Nazeeruddin, *Inorg. Chim. Acta.* 171, 213 **(1990)**; (b) F. De Angelis, S. Fantacci, A. Selloni, M. K. Nazeeruddin, and M. Graetzel, *J. Am. Chem. Soc.* 129, 14156 **(2007)**; (c) D. P. Hagberg, T. Marinado, K. M. Karlsson, K. Nonomura, P. Qin, G. Boschloo, T. Brinck, A. Hagfeldt, and L. Sun, *J. Org. Chem.* 72, 9550 **(2007)**; (d) M. K. Nazeeruddin, P. Pechy, T. Renouard, S. M. Zakeeruddin, R. Humphry-Baker, P. Comte, P. Liska, L. Cevey, E. Costa, V. Shklover, L. Spiccia, G. B. Deacon, C. A. Bignozzi, and M. Graetzel, *J. Am. Chem. Soc.* 123, 1613 **(2001)**.

**24.** N. Terasaki, T. Akiyama, and S. Yamada, *Langmuir* 18, 8666 **(2002)**.

**25.** X. Fang, T. Ma, G. Guan, M. Akiyama, and E. Abe, *J. Photochem. Photobio. A: Chem.* 164, 179 **(2004)**.

**26.** R. Jose, A. Kumar, V. Thavasi, and S. Ramakrishna, *Nanotechnology* 19 **(2008)**.

**27.** T. Miyasaka and K. Koyama, *Electrochem* 68, 865 **(2000)**.

**28.** A. D. Richards and A. Rodger, *Chem. Soc. Rev.* 36, 471 **(2007)**.

**29.** K. L. Fuller and S. G. Roscoe, *Protein Struct. Funct. Relat. Foods* 143 **(1994)**.

**30.** C. Fan, X. Hu, G. Li, J. Zhu, and D. Zhu, *Anal. Sci.* 16, 463 **(2000)**.

**31.** S. G. Roscoe, K. L. Fuller, and G. Robitaille, *J. Colloid Interface Sci.* 160, 243 **(1993)**.

**32.** W. S. Shin, S. C. Kim, S.-J. Lee, H.-S. Jeon, M.-K. Kim, B. V. K. Naidu, S.-H. Jin, J.-K. Lee, J. W. Lee, and Y.-S. Gal, *J. Poly. Sci., Part A: Poly. Chem.* 45 1394 **(2007)**.

**33.** A. Kay and M. Graetzel, *J. Phys. Chem.* 97, 6272 **(1993)**.

**34.** Amao and T. Komori, *Biosens. Bioelectron.* 19, 843 **(2004)**.

**35.** J. Shin, P. Bhattacharya, J. Xu, and G. Varo, *Opt. Lett.* 30 335 **(2005)**.

**36.** C. Nicolini, V. Erokhin, S. Paddeu, C. Paternolli, and M. K. Ram, *Biosens. Bioelectron.* 14, 427 **(1999)**.

**37.** Submitted to Biochemistry for review (2008).

**RESEARCH ARTICLE**